

Supplemental Table 1

Gene Symbol	FDR corrected p-value
<b>PLOD1</b>	4.52E-18
PDK1	6.77E-18
<b>CSRP2</b>	4.42E-17
<b>PFKP</b>	1.23E-14
MSH2	3.79E-13
NARF_A	5.56E-13
<b>ADFP</b>	5.56E-13
FAM13A1	1.56E-12
FAM29A_A	1.22E-11
CA9	1.54E-11
NDRG1_A	4.92E-11
GNRH1_A	1.08E-09
SOX4	7.17E-09
DDIT4	1.77E-08
SLC2A1_A	6.25E-08
SULT4A1	1.08E-07
PLOD2	1.49E-07
BRCA2	4.99E-07
PPFIA4	2.15E-06
CXCR4	2.52E-06
<b>ADM</b>	2.58E-06
LDHC	2.59E-06
NAV2	4.34E-06
PCTK3_A	6.04E-06
ANGPTL4	7.12E-06
DPYSL2	2.47E-05
PLXNB3_A	3.01E-05
IGFBP3	4.56E-05
<b>C10orf10</b>	4.59E-05
FBXO32_A	6.21E-05
SLC1A6	6.63E-05
EXOSC4	5.91E-05
SLC6A8	6.63E-05
POU5F1	7.96E-05
GAL3ST1	0.000114566
<b>GPI</b>	0.000137954
PGK1_A	0.000150415
HK2	0.000227913
ZNF292	0.000229199
SLC2A3	0.000232976
<b>LOX</b>	0.000332667
<b>PLEKHA2</b>	0.000629301
SLC16A3	0.001231339
<b>WIPF1</b>	0.001268432
CEP2_A	0.001945606
PIAS2	0.00225761
FLJ10415	0.002958248
KIAA1285	0.003436991
KIAA0779_A	0.017084379
DPYSL4	0.017084379
ARRDC3	0.017084379
E2-230K	0.032204839
PPL_A	0.041480863
FGF11	0.042200405
THOP1	0.048567902

## Supplementary figure legends

**Supplemental Table 1. HIF1A-target genes upregulated in TNBC patients.** Genes of the hypoxia signature significantly upregulated in TNBC samples compared to all other breast cancer sub-types and normal samples within 547 TCGA breast cancer samples. Genes highlighted in bold significantly correlate with *PML* expression.

**Figure S1. *PML* transcription is regulated by HIF1A (A-B)** RT-PCR analysis of *PML* (left) and *VEGF* (right) mRNA expression in NIH-3T3 (A) and HEK-293 (B) cells stably transduced with *shCTRL* (white dots) or *shHIF1A* (grey dots) and treated with deferoxamine (DFO) relative to expression levels in untreated cells. Data represent mean values  $\pm$  SEM of three independent experiments,  $\ast=p<0.05$ ,  $\ast\ast=p<0.01$ ,  $\ast\ast\ast=p<0.001$ . (C) Schematic representation of murine and human *PML* promoter reporter constructs (depicted not in scale). Predicted HRE sequences identified by MatInspector and PROMO programs are depicted by lines and numbers, human HRE#2 is conserved in mouse. (D-E) Left: luciferase reporter assays of *PML* promoter activity in NIH-3T3 (D) and HEK-293 (E) cells transfected with increasing concentrations of stable *HIF1A*; right: luciferase reporter assays of *PML* promoter activity in *shCTRL* (white dots) or *shHIF1A* (grey dots) NIH-3T3 (D) and HEK-293 (E) cells treated with DFO for the indicated periods of time. Data represent mean values  $\pm$  SEM of three independent experiments,  $\ast=p<0.05$ ,  $\ast\ast=p<0.01$ ,  $\ast\ast\ast=p<0.001$ . Luciferase activity is normalized to Renilla activity and expressed as fold induction relative to untreated cells. Student's two-tailed t-test was used to determine statistical significance except in panels D and E, where statistical analysis

was performed using 1-way ANOVA ( $p = 0.0013$  and  $0.0006$  respectively) followed by Tukey's post-hoc multiple comparison test.

**Figure S2. Regulation of *PML* expression by HIF1A in breast cancer cell lines.**

(A) RT-PCR analysis of the indicated genes in SUM-159 (top) and BT-549 (bottom) TNBC cells stably transduced with a control shRNA (white dots) or a *HIF1A* shRNA (grey dots). Data represent mean values  $\pm$  SEM of three independent experiments; \*\*= $p < 0.01$ , \*\*\*= $p < 0.001$ . (B) RT-PCR analysis of the indicated genes in MDA-MB-361 (top) and ZR-75-30 (bottom) non-TNBC cells stably transduced with a control shRNA (white dots) or a *HIF1A* shRNA (grey dots). Data represent mean values  $\pm$  SEM of three independent experiments; \*\*\*= $p < 0.001$ . (C) Fold enrichment over IgG levels normalized on gene body levels of DNA immunoprecipitated by control IgG (white dots) or anti-HIF1A antibody (grey dots) and amplified with primers spanning the promoter region of *PML* gene in the indicated non-TNBC cells. Data represent mean values  $\pm$  SEM of three independent experiments. Student's two-tailed t-test was used to determine statistical significance.

**Figure S3. *PML* silencing with different shRNA constructs leads to specific regulation of HIF1A-target genes.**

(A) RT-PCR analysis of *PML* expression in the indicated cell lines stably transduced with a control shRNA (white dots) or a *PML* shRNA (red dots). Data represent mean values  $\pm$  SEM of three independent experiments; \*\*= $p < 0.01$ , \*\*\*= $p < 0.001$ . (B) Immunoblot of PML protein expression in the indicated cell lines upon *PML* silencing with two shRNA constructs against *PML*.  $\beta$ -actin is used as loading control. (C) RT-PCR analysis of *CA9* (left) and *GLUT1* (right) levels in MDA-MB-231, SUM-159 and BT-549 TNBC cells stably

transduced with a control shRNA (white dots), shRNA against *HIF1A* (grey dots) or shRNA against *PML* (red dots). Data represent mean values  $\pm$  SEM of three independent experiments,  $*=p<0.05$ ,  $***=p<0.001$ . **(D-F)** RT-PCR analysis of the indicated genes in MDA-MB-231 **(D)**, SUM-159 **(E)** and MCF7 **(F)** cells stably transduced with a control shRNA (white dots) or an shRNA against *PML* (shPML#2, orange dots). Data represent mean values  $\pm$  SEM of three independent experiments,  $*=p<0.05$ ,  $**=p<0.01$ ,  $***=p<0.001$ . **(G)** Wound healing assays of the indicated cell lines stably transduced with a control shRNA (white dots) or *PML* shRNA#2 (orange dots). Data are expressed as wound area reduction compared to control cells of three independent experiments,  $*=p<0.05$ . **(H)** Invasion assays in the indicated cell lines stably transduced with a control shRNA (white dots) or *PML* shRNA#2 (orange dots). Data represent the number of cells per 20x field that invaded matrigel-coated transwells of three independent experiments,  $*=p<0.05$ . All quantitative data represent means  $\pm$  SEM. Student's two-tailed t-test was used to determine statistical significance.

**Figure S4. PML binds the regulatory regions and not the gene bodies of HIF1A-dependent metastatic genes.** **(A)** Schematic representation of enhancer and promoter regions of the indicated genes. Blue boxes indicate PML occupancy derived from ChIP-Seq experiments reported by the ENCODE project. Transcription start sites are indicated by black vertical lines, and direction of transcription is indicated in black arrows. Arrowheads indicate the position of primer sets used in ChIP experiments. **(B)** Fold enrichment over normalized IgG levels of DNA immunoprecipitated by control IgG (white dots) or PML (dark grey dots) antibodies and amplified with primers spanning either the regulatory regions or the gene body of the indicated genes

in MDA-MB-231 cells. Data represent mean values  $\pm$  SEM of three independent experiments; \* $p < 0.05$ , \*\*\*= $p < 0.001$ . Student's two-tailed t-test was used to determine statistical significance.

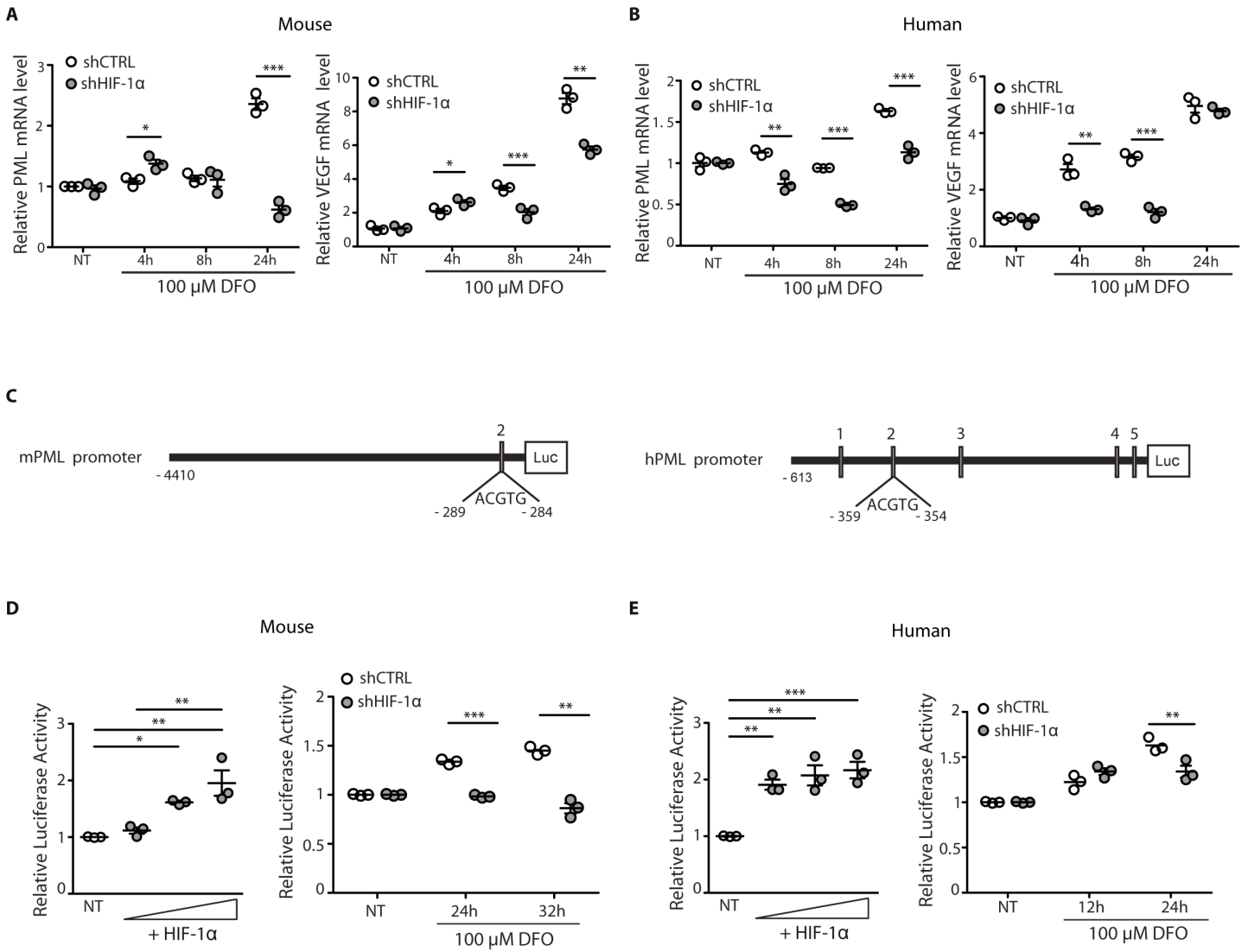
**Figure S5. PML and HIF1A-dependent metastatic genes are highly expressed in TNBC cell lines.** (A) Cell lines from the Cancer Cell Line Encyclopedia used in the comparative analysis of gene expression and distributed according to breast cancer sub-types. (B) Distribution of mRNA expression retrieved from the Cancer Cell Line Encyclopedia of the indicated genes normalized over *B actin* mRNA values across the indicated groups of cells lines: ER+, estrogen-positive (n=6); HER-2+, HER-2 receptor-positive (n=6); TNBC, triple-negative (n=20); \* $p < 0.05$ . 1-way ANOVA (p for PML and PLOD1=0.0497 and 0.0146 respectively) followed by Tukey's post-hoc multiple comparison test was used to determine statistical significance.

**Figure S6. Effect of PML silencing on proliferation and viability in representative breast cancer cell lines.** (A) Proliferation curves of the indicated cell lines stably transduced with a control shRNA (black line) or two different shRNA against *PML* (orange and red lines). Values represent ratios of cell numbers over cell numbers at day 0. Data represent mean values of three technical replicates of one representative experiment out of three with similar results. (B) Percentage of trypan blue positive cells in the indicated cell lines stably transduced with a control shRNA or two different shRNA against *PML* (white, orange and red dots) Data represent mean values  $\pm$  SEM of three independent experiments.

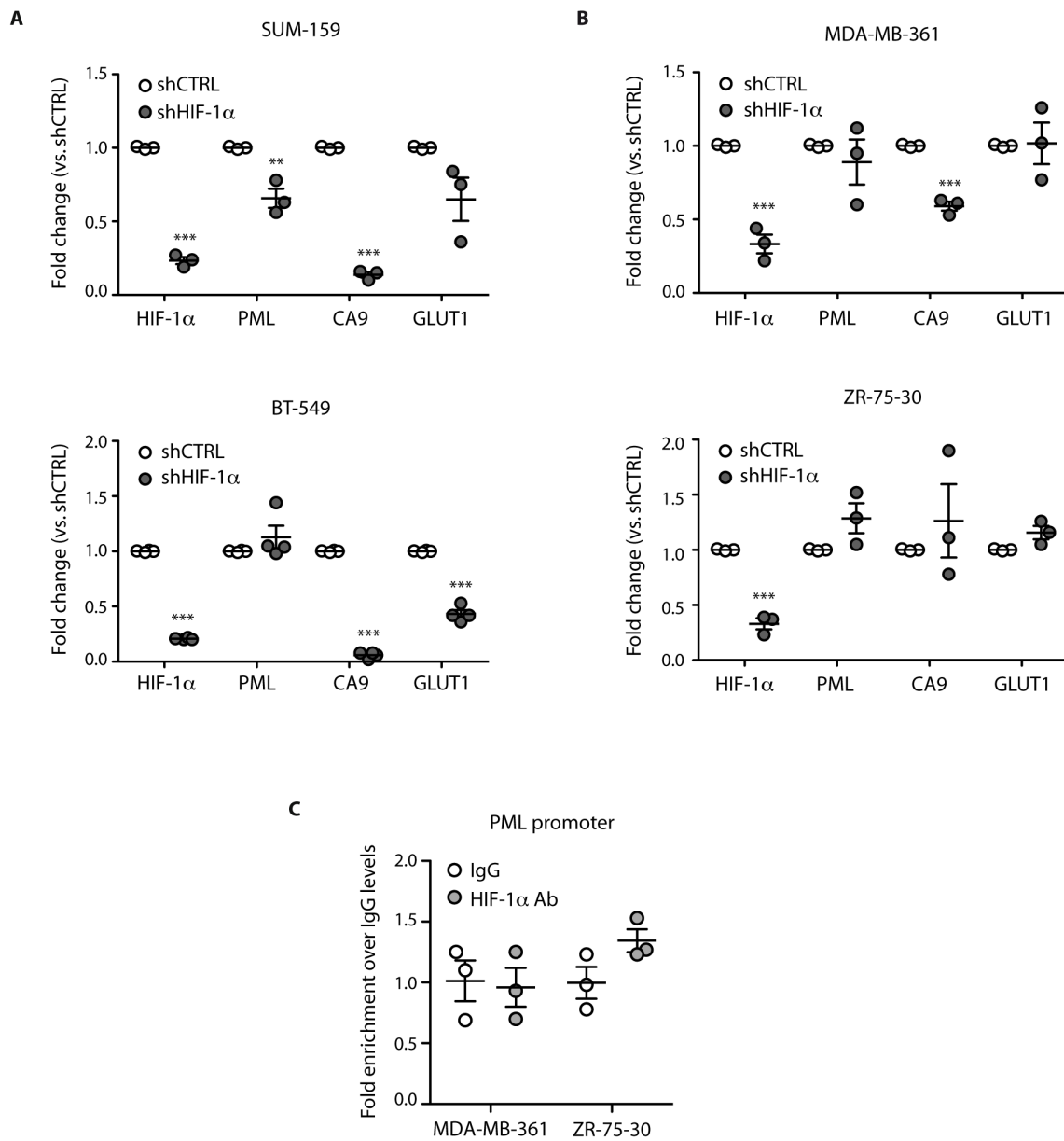
**Figure S7. *Pml* silencing regulates metastatic genes, migration and invasion in mouse TNBC cells.** (A) RT-PCR analysis of the indicated genes in mouse 4T1 cells stably transduced with a control shRNA (white dots) or shRNA against *Pml* (blue dots). Data represent mean values  $\pm$  SEM of three independent experiments,  $*=p<0.05$ ,  $***=p<0.001$ . (B) Wound healing assays of mouse 4T1 cells stably transduced with a control shRNA (white dots) or *Pml* shRNA (blue dots). Data are expressed as wound area reduction compared to control cells and represent mean values  $\pm$  SEM of three independent experiments,  $***=p<0.001$ . (C) Tumor volumes of 4T1 cells transduced with shCTRL or *Pml* shRNA (blue line) and implanted in fat pads. Data represent mean values  $\pm$  SEM;  $n=5$ ,  $**=p<0.01$ . (D) Lung metastases in mice described in (C). Number of metastatic foci per lung slide in the indicated animals. Data represent mean values  $\pm$  SEM,  $n=5$ ,  $*=p<0.05$ . Student's two-tailed t-test was used to determine statistical significance.

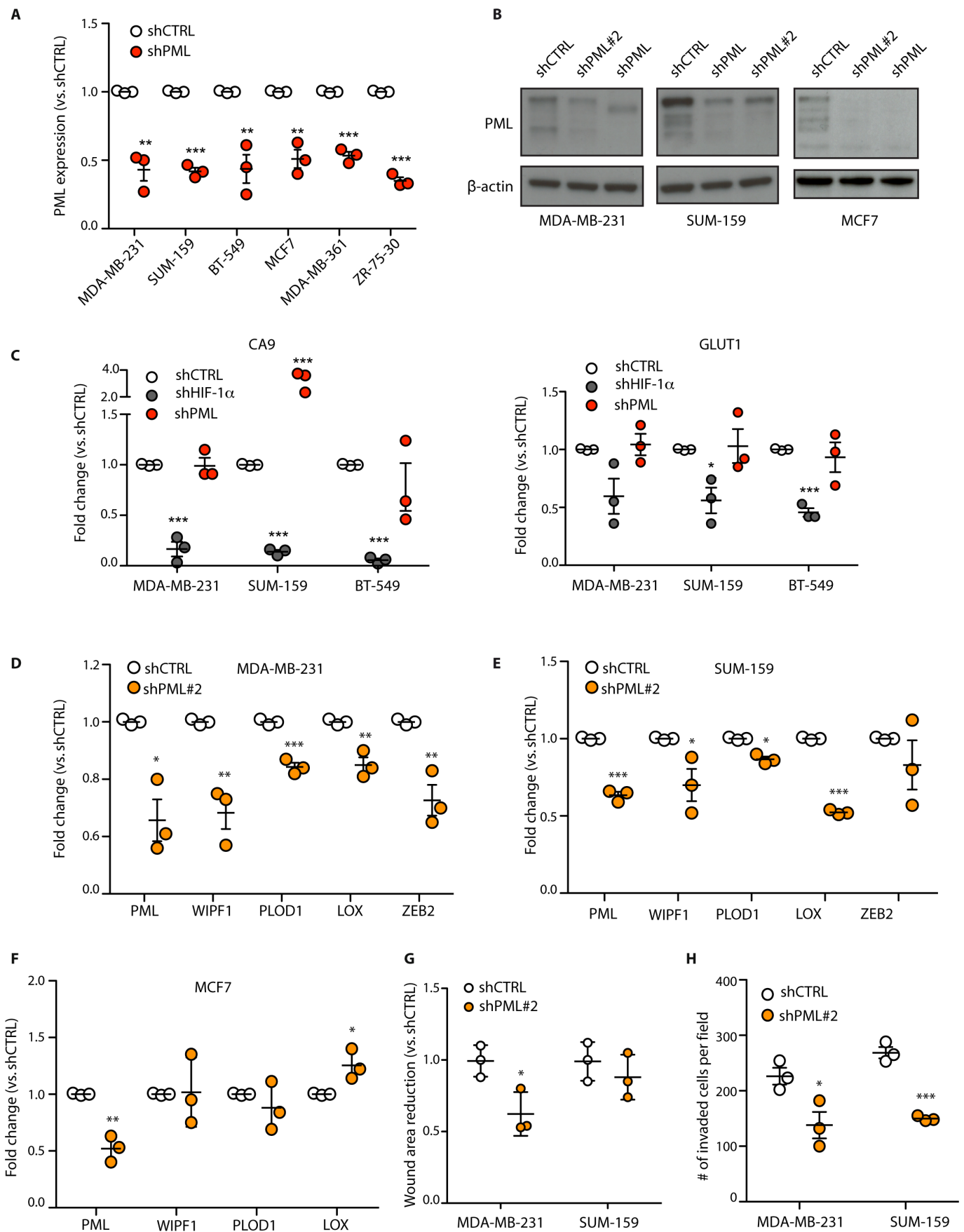
**Figure S8. Arsenic trioxide modulates PML expression and metastatic features in TNBC cells.** (A) Immunoblot of PML protein expression in the indicated cell lines either non-treated (NT) or upon treatment with arsenic trioxide at the indicated doses. Cropped blots are surrounded by a black line and retain important bands, B actin is used as loading control. (B) Number of trypan blue positive (red dots) or negative (black dots) cells counted after arsenic trioxide treatment in the indicated cell lines. Data represent mean values  $\pm$  SEM of three independent experiments. (C) RT-PCR analysis of the indicated genes in 4T1 mouse cells untreated (NT, white dots) or treated with the indicated doses of arsenic trioxide. Data represent mean values  $\pm$  SEM of three independent experiments,  $*=p<0.05$ ,  $**=p<0.01$ . (D) Wound healing assays of mouse 4T1 cells treated as in (C). Data are expressed as wound area

reduction compared to control cells and represent mean values  $\pm$  SEM of three independent experiments,  $*=p<0.05$ . (E) Invasion assays of 4T1 mouse cells treated as in (C). Data represent the number of cells per 20x field that invaded matrigel-coated transwells. Data represent mean values  $\pm$  SEM of three independent experiments,  $**=p<0.01$  (F) Left: tumor weights measured after sacrifice of animals described in Figure 5D. Data represent mean values  $\pm$  SEM,  $n=5$ . Right: PML immunohistochemistry in representative tumors untreated or treated with arsenic trioxide. Scale bar, 50  $\mu\text{m}$ . (G) Tumor weights measured after sacrifice of animals described in Figure 5F. Data represent mean values  $\pm$  SEM,  $n=5$ . Student's two-tailed t-test was used to determine statistical significance except in panel D, where statistical analysis was performed using 1-way ANOVA ( $p=0.0119$ ) followed by Tukey's post-hoc multiple comparison test.





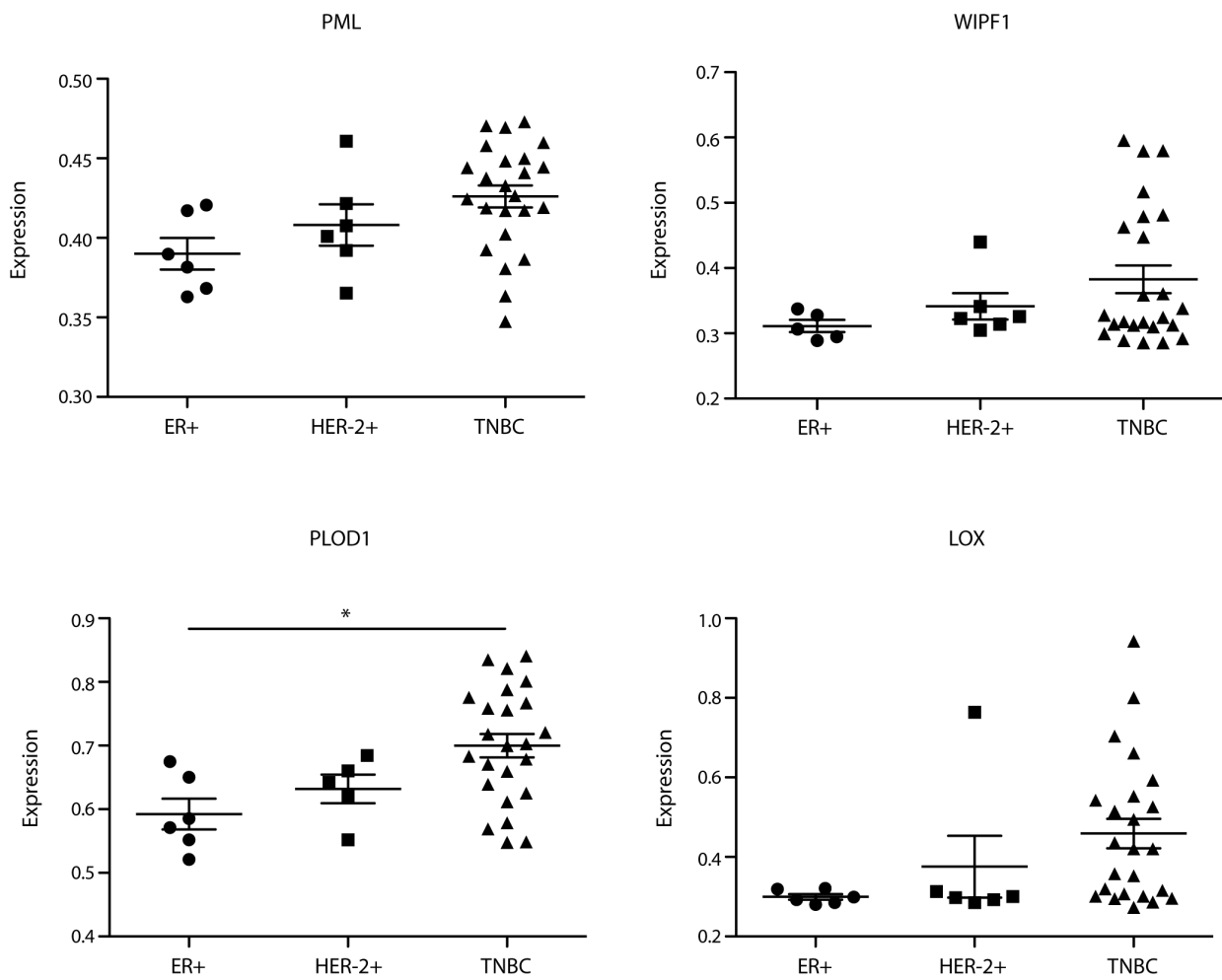


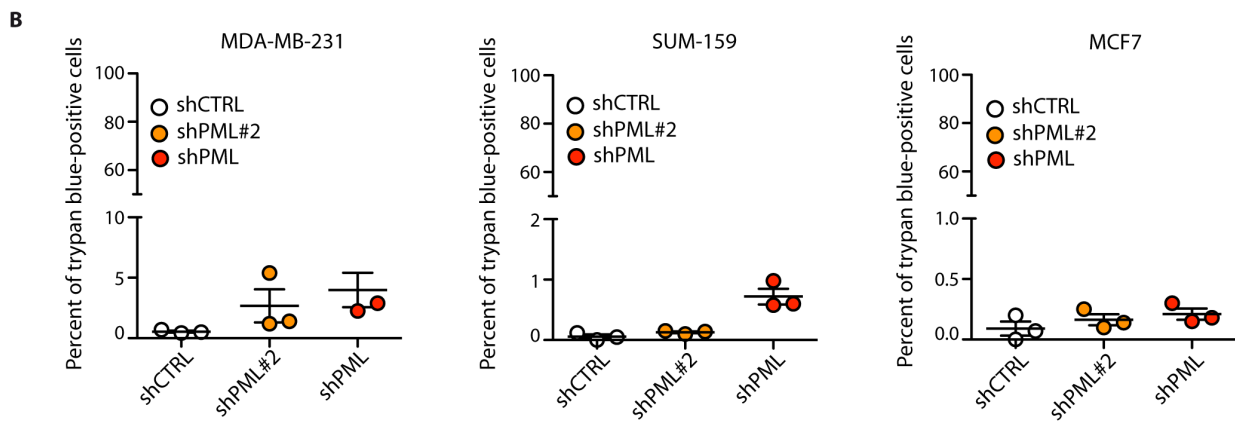
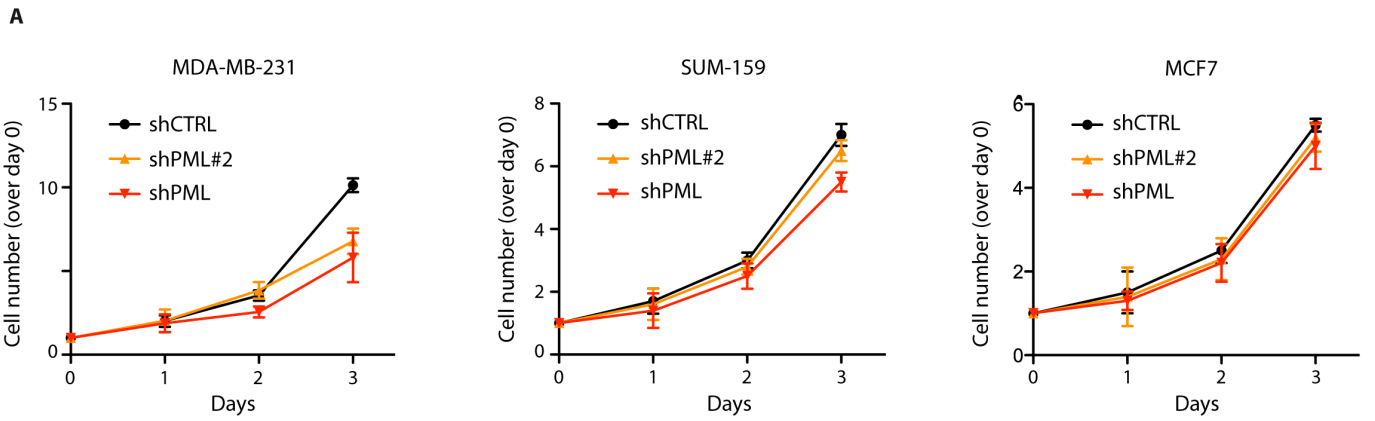


A

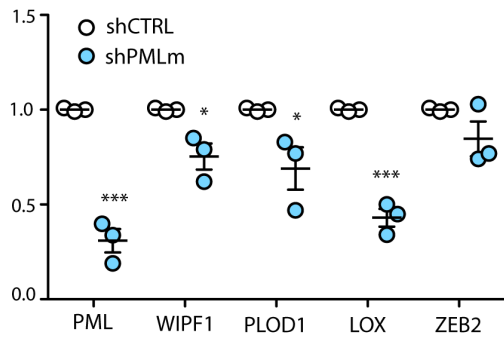
<b>ER+</b>	BT483, EFM19, HCC1428, HCC1500, MCF7, MDAMB134VI
<b>HER2+</b>	HCC202, HCC1419, HCC1569, HCC1954, HCC2218, SKBR3
<b>TNBC</b>	HCC2157, HCC1599, HCC1937, HCC1143, MDAMB468, HCC38, CAL851, HCC70, HCC1806, HDQP1, DU4475, HCC1187, BT549, CAL51, CAL120, MDAMB157, MDAMB436, MDAMB231, HS578T, CAL148, MDAMB453, BT20, HCC1395, MDAMB175VII

B

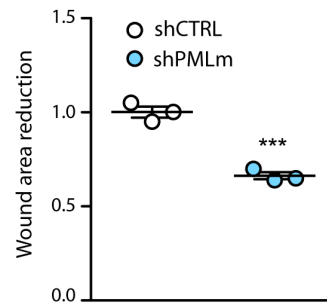




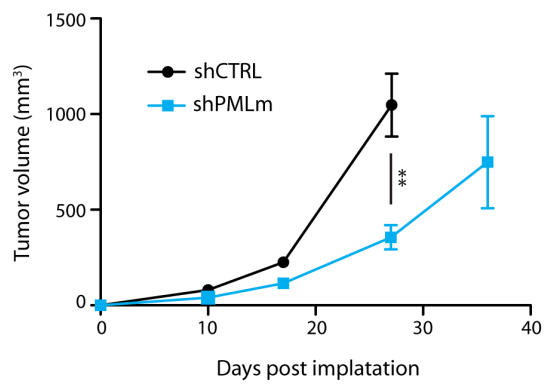
**A**



**B**



**C**



**D**

